International Journal of Modern Physics and Application
2015; 2(6): 105-109
Published online December 11, 2015 (http://www.aascit.org/journal/ijmpa)
ISSN: 2375-3870

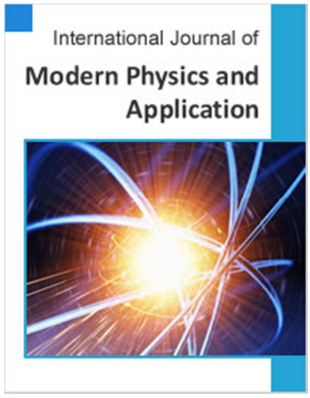

Keywords
N-doped,
Band Gap,
Photoelectrical Properties,
Nanoparticle

Received: October 23, 2015
Revised: November 9, 2015
Accepted: November 11, 2015

The Effect of Pressure and Band Gap Theoretical Study in N-doped TiO_2 Nanoparticles

Xin Wang[1, 2, *], Hongkun Zhang[1], Tao Jiang[1], Yanan Li[1], Liangsheng Qiang[2]

[1]Department of Applied Chemistry, East University of Heilongjiang, Harbin, P. R. China
[2]Department of Applied Chemistry, Harbin Institute of Technology, Harbin, P. R. China

Email address
wangxin5569@163.com (Xin Wang)

Citation
Xin Wang, Hongkun Zhang, Tao Jiang, Yanan Li, Liangsheng Qiang. The Effect of Pressure and Band Gap Theoretical Study in N-doped TiO_2 Nanoparticles. *International Journal of Modern Physics and Application*. Vol. 2, No. 6, 2015, pp. 105-109.

Abstract
As part of our efforts to find a way to control the concentration of N-doped TiO_2, TiN_xO_y powers are prepared by a device of our own design. Nanomaterials are generated using N-doped TiO_2 material with their concentrations by adjusting the amount of NH_3 under middle pressure. N-doped TiO_2 particles are characterized under the reaction conditions at different middle pressure. Experimental results indicate that the band gap of semiconductor has been narrowed by increasing of the concentration of N-doped TiO_2. It can therefore be concluded that the synthesis route we found through this study is an effective way to adjust the relationships between the concentration and the band gap of the N-doped TiO_2 nanomaterials.

1. Introduction

Since Grätzel [1] developed solar cells based on the nanocrystalline TiO_2 electrode, dye sensitized solar cells (DSCs) have attracted much attention for their relatively low cost and high photoelectrical property. [2–5] A variety of methods have been devised to fabricate nanoscale TiO_2 film electrode to obtain high energy conversion efficiency for solar cells, such as replacing with liquid electrolyte, [6] doping atoms in TiO_2, [7] improving the performance of dye, [8] etc. Considerable efforts have been directed to the synthesis of doped-TiO_2 with the optical absorption edge redshifted towards the visible light region. Nitrogen-doped TiO_2 has been investigated by experimental and theoretical approaches [9–13] since it was proposed by R. Asahi. [14] In recent years, a variety of methods have been reported about the visible light photocatalysis of N-doped TiO_2, such as the sputtering of TiO_2 target in an N_2/Ar gas mixture, [15] oxidation of TiN, [16] hydrolysis of TiO_2 tetrachloride with a nitrogen containing base, [17] amination of TiO_2 particles, [18] nitrogen ion implantation, [19] chemical vapor deposition, [20] sol–gel, [21] and decomposition of N-containing metal organic precursors, [22] etc. Among the abundant reasonable designs, Tingli Ma [23] reported N-doped TiO_2 electrode could be used to improve the overall conversion efficiency (η) in 2005. However, these methods showed that there was no effective way to adjust the relationships between the concentration and the band gap of the N-doped TiO_2. As part of our efforts to find a way to control the composition of N-doped TiO_2, we designed a device to generate TiN_xO_y powders used NH_3 as gaseous precursor. The photoelectrical properties of N-doped TiO_2 electrode are characterized by XPS, XRD, Raman, SEM, TPV and SPS analysis under the reaction conditions at different reaction pressure. However, when the interfacial electrons

are located in the nanoscale environments, their transferring behavior associated with the spatial heterogeneities become complex. Herein, the research has also offered photoelectrochemical analysis to prove the relationships between the concentration and the band gap of the N-doped TiO_2 nanomaterials.

2. Experimental Methods

Materials. Titanium isopropoxide is purchased from Aldrich Chemical Company.

Preparation. Nanocrystalline titania powders were synthesized by hydrothermal method with titanium isopropoxide used as titanium source. Then, the powder was treated at different temperature in the atmosphere of NH_3 gas at different pressure in a sealed steel autoclave designed by ourselves.

After being cooled to room temperature, polyethylene glycol (PEG, molecular weight (MW) of 600, made in China) was added to TiN_xO_y slurry in ethanol solvent at a proportion of 10% powers. After that, films on FTO glasses were prepared by screen-printed method and gradually sintered at 450°C under dry air for device fabrication.

As shown in Figure 1, the samples were prepared in a sealed stainless steel chamber (part 1). The gas of NH_3 (99 %, part 3) flowed to the chamber via a device (part 2) that absorbed impurities in NH_3. The heater power did not launch until pressure reached to the predetermined values. When the temperature reached to 400°C, the preservation time sustained for 24 h, respectively. Conditions for the thermal treatment of powders were investigated by changing pressure. Regarding to simplify and reduce the number of variables, three sets of remarkable sintering routes on the film composition are proposed as follows: 400°C, 1.0 MPa, 24 h; 400°C, 0.6 MPa, 24 h; 400°C, 0.2 MPa, 24 h.

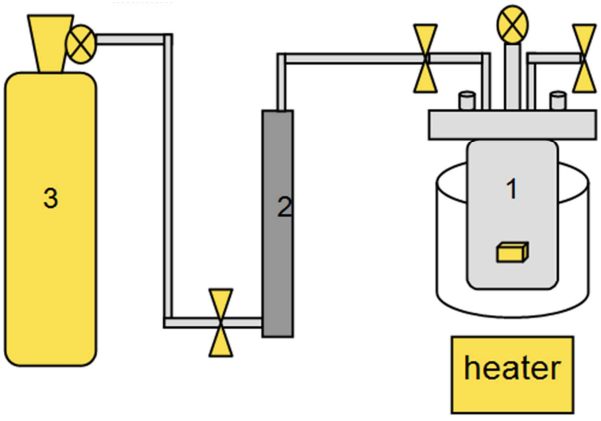

Figure 1. *Apparatus for surface-treatment of N-doped TiO_2 powders.*

Characterization. The phase structure of the plasma treated powders was characterized by X-ray diffraction (JDX-3530M, Japan) using Ni filtered Cu Kα radiation. The X-ray photoelectron spectroscopy with the Al Kα source generated by Thermo ESCALAB-250 spectrometer, equipped with ultrahighvacuum(UHV) at 3.5×10^{-7} Pa. The surface morphology of the raw and the processed powders was observed using a scanning electron microscope (SEM S-IRION, American-FEI Company; Hitachi S-4800). The Powder Raman spectra were collected on RFS 100FT-Raman spectrometer, Bruker Company, with a optical excitated wavelength at 1064 nm laser and exported electric power at 20mW. The SPS instrument was assembled at Jilin University, monochromatic light was obtained by passing light from a 500 W xenon lamp (CHF-XQ500W, China) through a double-prism monochromator (SBP300, China). The transient photovoltage (TPV) tests were excited with a laser radiation pulse (wavelength of 355 nm and pulse width of 5 ns) from a third-harmonic Nd:YAG laser (Polaris II, New Wave Research, Inc.). The slit widths of entrance and exit were 2 and 1 mm, respectively. A lock-in amplifier (SR830, USA), synchronized with a light chopper (SR540, USA), was employed to amplify the photovoltage signal.

3. Results and Discussion

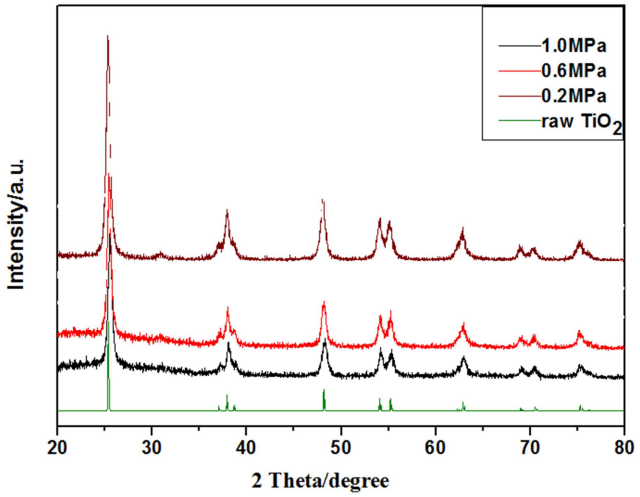

Figure 2. *XRD patterns of raw TiO_2 and N-doped powders at different pressures.*

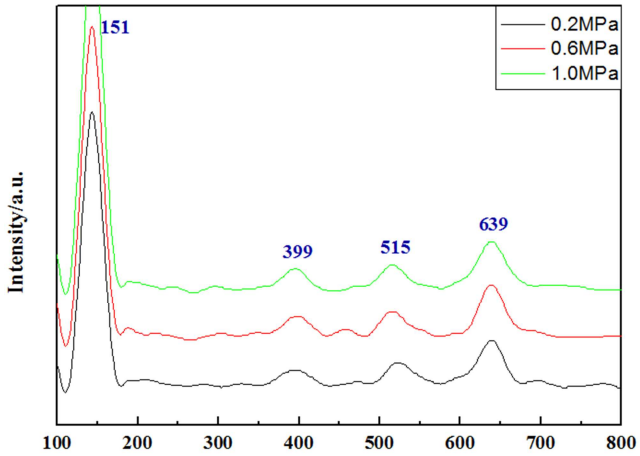

Figure 3. *Raman spectra of raw TiO_2 and N-doped TiO_2 powders at different pressures.*

As shown in the supporting information, the XRD patterns of TiN_xO_y indicate that the pressure is no evidence effective to the change of phase composition compared with the temperature. The crystal structure of nitrogen-doped TiO_2 is in general similar to that of TiO_2, as shown in Figure 2. The strong absorption diffraction peaks are assigned to the anatase-type in a temperature of 400°C. Those results are in good agreement with the results of Raman Spectroscopy. Figure 3 shows five active fundamental modes around 151 (E_g), 204 (E_g), 399 (B_{1g}), 515 (A_{1g}, B_{1g}), and 639 cm^{-1} (E_g), which belong to the anatase phase.

However, the nanostructure is not the only determinant element for the differences between TiN_xO_y nanomaterials. Whether the concentration of nitrogen-doped nanomaterials plays an important role is discussed by XPS results. Table 1 demonstrates that a slight narrowing of forbidden-gap emerged by increasing the concentrations of the Nitrogen doped in samples. Moreover, it also represents the general relationships involved the concentration of N-doped TiO_2 and band gap in TiO_2 films.

Table 1. *Comparation in the concentration and band gap of N-doped TiO_2 samples.*

	400°C, 24 h, 0.2 MPa	400°C, 24 h, 0.6 MPa	400°C, 24 h, 1.0 MPa
N-doped concentration/% (XPS)	0.87	0.60	0.46
Band gap/eV (SPS)	2.63	2.80	3.08

As shown in Figure 4, the results represent two differential peaks of N that are centered at 396 and 400 eV, respectively. The 400 eV band is attributed to molecularly chemisorbed dinitrogen γ-N_2. The 396 eV peak is assigned as atomic β-N bonded to Ti, that is, when N substitutionally replaced O, sites are associated with atomic N.

It is reported that it needs some requirements to achieve visible-light-activity for N-doped TiO_2: (i) doping should produce states in the band gap of TiO_2 that absorb visible light; (ii) the dopant states of doped TiO_2 should form a narrow N 2p band above the valence band of TiO_2 to ensure photoreductive activity.

Table 1 indicates that the concentration of N-doped TiO_2 has been increased with less pressure. The results also provide that high concentration in N-doped TiO_2 could construct with a higher visible light activity. It is difficultly for N atom to insert TiO_2 crystal lattice due to its metamorphosing under the pressure of gas-solid reaction. With increasing of pressure, the movement of gasified molecule emerged excitedly, which was no benefit for N indwelled in TiO_2 lattice, therefore the concentration of N-doped TiO_2 decreased.

During N replaced O in TiO_2 lattice, NH_3 played a role as a kind of reducer, which attached itself to adjusting the quantity balance of oxygen vacancies (V_{Os}) and dopant N. Due to the increase of x in TiN_xO_y, V_{Os} act as recombination centers for e^- and h^+, which led to a lower visible light activity. In this case, suitable proportion between V_{Os} and dopant N determined the photoelectrical property of N-doped TiO_2.

On irradiating with visible light, the quantum yields increased with the concentration of Nitrogen, suggesting that the intragap states should sufficiently overlap with the band states of TiO_2. This result led to photoexcited carriers (e^-) transfer to reactive sites at the TiO_2 surface within their lifetime.

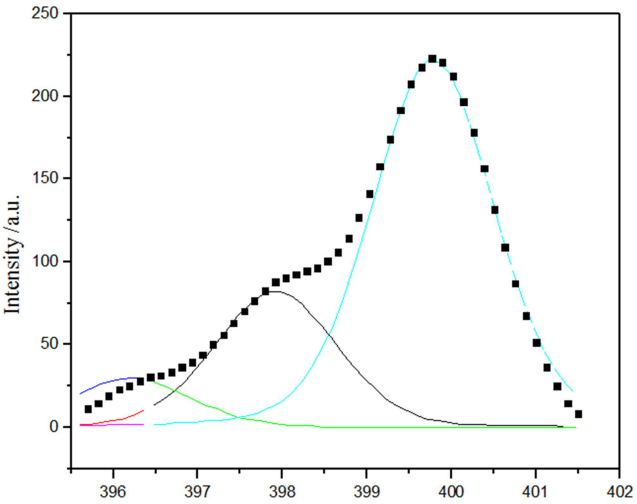

Figure 4. *The XPS spectra of N_{1s} core-level of N-doped TiO_2 powders treated at 400°C with 24 h at 1.0 MPa.*

The surface photovoltage spectrum (SPS) method is commonly applied to nanoparticles for their photoelectrical properties, which is a well established contactless technique for surface state distribution. As shown in Figure 5, the SPS analysis demonstrates that one typical characteristic response band closed from 400 to 550 nm, which originates from the band-band electron transition of N-doped band. The presence of the signal is probably caused by the N-doped band, which is benefit for the visible light response range broadened. The band gap is calculated from formula: E_{gap}(eV)=1240/λ_{max}(nm), where E_{gap} is the band gap and λ_{max} represents the edge of maximal response absorption band. This phenomenon provides clear evidence that higher concentration in N-doped TiO_2 could construct with narrower band gap.

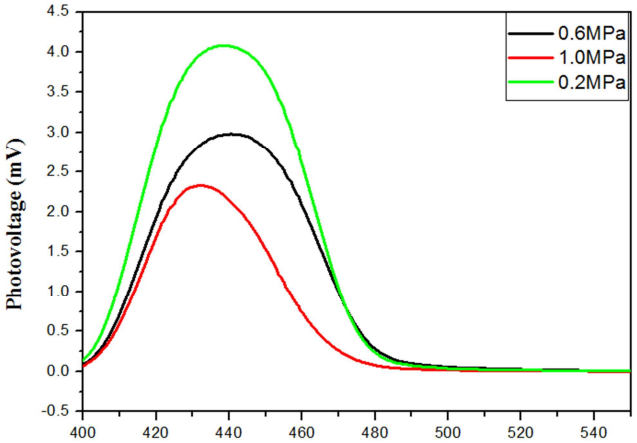

Figure 5. *SPS of N-doped samples.*

In addition, it is also observed that the surface morphology is related to the amount of N doped. The grain sizes in such

samples are gradually increasing from 10 up to 50 nm after sintering in a temperature of 400°C for 24 h according to SEM micrographs. Figure 6 illustrates that the average size of nanocrystal has become smaller and more equal after thermal treatment. Further increase of the concentration of N doped decreases the sizes of grains. And else, the approximate nanoparticles diameter changes under different reaction conditions. Based on earlier studies, these results can be explained by the theory that the rate of crystal growth is relevant to the environment outside, such as pressure.

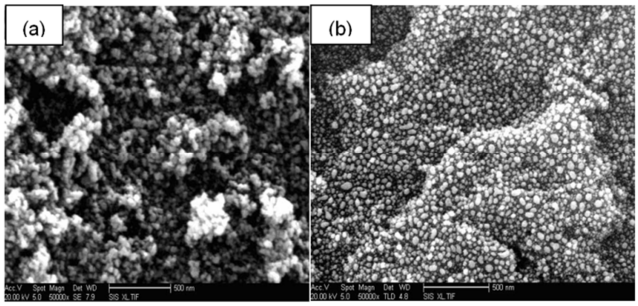

Figure 6. *SEM micrographs of (a) raw TiO_2: (b) N-doped TiO_2 powders digested at 400°C for 24 h under 1.0 MPa. The N-doped particles are approximate 20 nm with sphere-like ones.*

The transient photovoltage (TPV) technique is an useful method for the investigation of dynamic behavior of photo-induced charge carriers (PICCs) in semiconductor materials, which dominates the performance of the photoelectrical properties. We can directly obtain information about the charge dynamics, including generation, separation and recombination of photo-induced charges by TPV technique.

The photovoltage (PV) arises whenever light-induced excess charge carriers are separated in space. The excitation of excess carriers of charge is performed with photons of $h\nu > E_g$. The sign of the PV transients is positive. The positive sign implies that the photoexcited electrons move faster than holes towards the N-doped TiO_2/SnO_2: F interface. No PV signal could be detected for $h\nu < E_g$.

It is also considered the important effect of the recombination between injected carriers and holes in the charge transport. Figure 7 displays retardation due to the effect of recombination in TiO_2. The retardation of the transient PV in N-doped TiO_2 differs drastically from the material without N doped. The PV transients do not decay purely by exponent or logarithmic law. A lifetime of charge carriers could be introduced for exponential decay while the recombination of specially separated charge could be used to describe a logarithmic decay. The feature originated from the back diffusion of electrons. At the initial time, the large gradient induced by the injection produces finished the diffusion process of the injected electrons toward the back contact. This reverse gradient also produces back diffusion of the electrons to the region with high recombination probability, originating the fast decay in the SPV observed in Figure 7, in which the recombination is assisted by the diffusion. The gradient of excess electron and hole concentrations is caused by nonhomogeneous of the nature of N-doped TiO_2 sample.

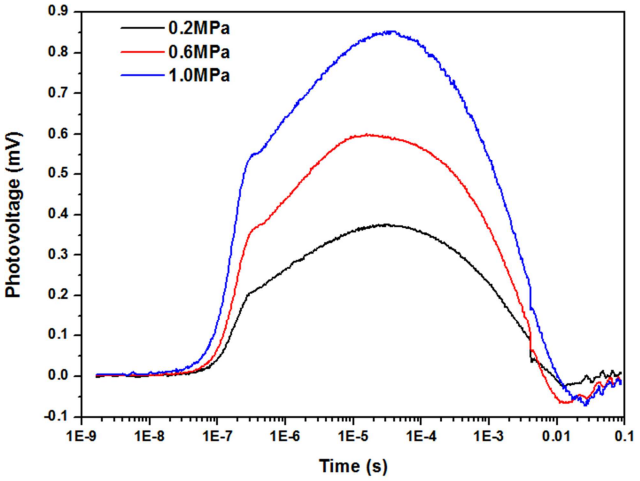

Figure 7. *The photovoltage transients of the particles (a) N-doped TiO_2 sample (b) TiO_2 sample without N atom; The wavelength and the intensity of the laser are 355 nm and 50 μJ, respectively.*

The narrowing of forbidden-gap leads to an increase of the amplitude of spectral PV and to a much stronger retardation of the PV transients. The retardation behavior of the PV transients changes dramatically after generation of N dopant band states. Since the optical band gap (E_g) of TiO_2 is 3.2 eV, excitation under 355 nm (photon energy $h\nu$ = 3.5 eV) leads to a band-to-band transition. Therefore, we can describe a sketch of energy band at the interface, which origins from the presence of intragap dopant states above the upper level of the VB band in TiO_2. (as shown in Figure 8) This fact indicates that the electrons transfer away from the injection region and diffuse to the high recombination region in the forbidden-gap, producing the fast decay observed at longer times.

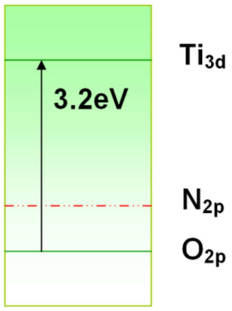

Figure 8. *The sketch of band states at the interface in N-doped TiO_2.*

Combining with experiment results above, it is safely concluded that band gap narrowed predominates the performance of photoelectrical properties than the effect of the recombination between injected carriers and holes in N-doped TiO_2 material.

4. Conclusion

As part of our efforts to find a way to control the concentration of N-doped TiO_2, TiN_xO_y powers are prepared by a device of our own design. Nanomaterials are generated

using N-doped TiO_2 material with their concentrations by adjusting the amount of NH_3 under middle pressure. Experimental results provide clear evidence that higher concentration of N-doped TiO_2 could construct with narrower band gap, as the red-shifted absorption edges originate from the presence of intragap dopant states above the upper level of the VB band. To sum up, it can therefore be concluded that the research has offered proof for the relationships between the concentration and the band gap of the N-doped TiO_2 nanomaterials. The grain sizes in N-doped TiO_2 film are controlled by the concentration of N-doped TiO_2, which are in the range of 10–50 nm. In terms of nanoparticles size, excellent anatase phase and suitable concentration of Nitrogen doped, all of them are controlled by different middle pressure. It is hoped to offer an effective way to adjust the relationships between the concentration and the band gap of the N-doped TiO_2 nanomaterials and find underline applications on solar cells and other photocatalical fields.

Acknowledgments

This work was supported by Youth Foundation of Heilongjiang Province of China (No. QC2012C088).

References

[1] O'Regan, B.; Grä tzel, M. *Nature* 1991, *353*, 737.

[2] Lopez-Luke, T.; Wolcott, A.; Xu, L. P.; Chen, S.; Wen, Z.; Li, J.; De La Rosa, E.; Zhang, J. Z. *J. Phys. Chem. C*. 2008, *112*, 1282.

[3] Ikeda, N.; Miyasaka, T. *Chem. Commun.* 2005, *5*, 1886.

[4] Wang, Z. S.; Huang, C. H.; Huang, Y. Y.; Hou, Y. J.; Xie, P. H.; Zhang, B. W.; Cheng, H. M. *Chem. Mater.* 2001, *13*, 678.

[5] O'Regan, B.; Lenzmann, F.; Muis, R.; Wienke, J. *Chem. Mater.* 2002, *14*, 5023.

[6] Bach, U.; Lupo, D.; Comte, P. *Nature* 1998, *395*, 583.

[7] Sun, H. Q.; Bai, Y.; Jin, W. Q.; Xu, N.P. *Sol. Energy Mater. & Sol. Cells*. 2008, *92*, 76.

[8] Gao, F.; Wang, Y.; Shi, D.; Humphry-Baker, R.; Wang, P.; Zakeeruddin, S. M.; Grätzel, M. *J. Am. Chem. Soc.* 2008, 130, 10720.

[9] Zhen-Yu Wu, Xing-Xing Xu, Bi-Cheng Hu, *Angewandte*, 2015, 54, 8179–8183.

[10] Livraghi, S.; Paganini, M. C.; Giamello, E.; Selloni, A.; Di Valentin, C.; Pacchioni, G. *J. Am. Chem. Soc*. 2006, *128*, 15666.

[11] Cheung, S. H.; Nachimuthu, P.; Engelhard, M. H.; Wang, C. M.; Chambers, S. A. *Surface Science* 2008, *602*, 133.

[12] W Yang, G Tan, J Huang, H Ren. *Ceramics International*, 2015, 41(1):1495–1503.

[13] In, S.; Orlov, A.; Berg, R.; Garcia, F.; Pedrosa-Jimenez, S.; Tikhov, M. S.; Wright, D. S. *J. Am. Chem. Soc*. 2007, *129*, 13790.

[14] Asahi, R.; Morikawa, T.; Ohwaki; Aoki, K.; Taga, Y. *Science* 2001, *293*, 269.

[15] Asahi, R.; Morikawa, T. *Chemical Physics*. 2007, *339*, 57.

[16] Batzill, M.; Morales, E. H.; Diebold, U. *Chemical Physics*. 2007, *339*, 36.

[17] Chen, S. F.; Chen, L.; Gao, S.; Cao, G. Y. *Chem. Phys. Lett*. 2005, *413*, 404.

[18] Fang, X. M.; Zhang, Z. G.; Chen, Q. L.; Ji, H. B.; Gao, X. N. *J. Solid State Chem*. 2007, *180*, 1325.

[19] Chen, H.; Nambu, A.; Wen, W.; Graciani, J.; Zhong, Z.; Hanson, J. C.; Fujita, E. *J. Phys. Chem. C*. 2007, *111*, 1366.

[20] Randeniya, L. K.; Bendavid, A.; Martin, P. J.; Preston, E. W. *J. Phys. Chem. C*. 2007, *111*, 18334.

[21] Pomoni, K.; Vomvas, A.; Trapalis, C. *Thin Solid Films*. 2008, *516*, 1271.

[22] Li, J. G.; Yang, X.; Ishigaki, T. *J. Phys. Chem. B*. 2006, *110*, 14611.

[23] Ma, T.; Akiyama, M.; Abe, E.; Imai, I. *Nano Lett*. 2005, *5*, 2543.